Turkish Journal of Electrical Engineering & Computer Sciences

http://journals.tubitak.gov.tr/elektrik/

Research Article

Turk J Elec Eng & Comp Sci
(2015) 23: 1431 – 1448

doi:10.3906/elk-1305-84

Study of MAC routing in the BPLC P1901 access network: fixed vs. adaptive approach

Asmir GOGIC[1], Aljo MUJCIC[1], İsmail Hakkı ÇAVDAR[2], Matej ZAJC[3], Nermin SULJANOVIC[1,*]

[1]Department of Communications, Faculty of Electrical Engineering, University of Tuzla, Bosnia and Herzegovina
[2]Department of Electronics, Karadeniz Technical University Trabzon, Turkey
[3]Digital Signal, Image, and Video Processing Laboratory, Faculty of Electrical Engineering, University of Ljubljana, Slovenia

Received: 10.05.2013 • **Accepted/Published Online:** 16.09.2013 • **Printed:** 28.08.2015

Abstract: In this paper we propose an improved adaptive media access (MAC) layer routing algorithm for the broadband power line communication (BPLC) access network founded on the fixed basic approach routing algorithm, which is integrated within the IEEE P1901 standard. The proposed adaptive algorithm incorporates a new dynamically scaled threshold for the selection of the next hop station based on the information from the physical layer. Furthermore, the procedures for the route and the time allocation modifications during the connection setup and later adjustments are developed. Simulation of the new adaptive and existing fixed routing algorithm is performed on the model of a realistic BPLC network using the OMNeT++-based BPLC cross-layer simulator BPlcSim. The simulation results showed that the adaptive routing algorithm outperforms the fixed routing in all aspects, since each station can perform routing functions and make the selection of the most reliable next hop station.

Key words: Power line communications, media access protocol, cross-layer simulation, smart grid, routing and repeating

1. Introduction

The power line communication (PLC) technology is a promising path for the implementation of the smart grid communication infrastructure since it utilizes power grids for communication purposes [1]. In other words, PLC is natively incorporated into the smart power grid [2]. Communication infrastructure for the BPLC network within low-voltage (LV) and medium-voltage (MV) access networks at the media access (MAC) layer and the physical (PHY) layer is defined by the newly adopted IEEE P1901 standard [3]. The LV access network infrastructure represents a shared communication medium, which is characterized as a hostile environment for data transmission due to the strong signal attenuation and extensive fluctuations in the noise level [4]. This means that some of the stations in the BPLC network will not be able to directly communicate with one another. Despite the fact that the physical topology of the BPLC network is unchanged, the stations in the logical network will exhibit a characteristic of mobility. In order to cope with such a problem, it is necessary to provide the mechanism for the determination of the path between the source and destination.

This paper presents an improved adaptive MAC routing algorithm for the LV BPLC access network aligned with the IEEE P1901 standard [3]. The adaptive routing algorithm utilizes the infrastructure of the

*Correspondence: nermin.suljanovic@untz.ba

fixed routing algorithm, which is natively incorporated in the IEEE P1901 standard. It is based on the concept presented in [5] where each station can perform the functions of a router. Additionally, the adaptive routing algorithm employs the interaction between the MAC and the PHY layer in order to select the most reliable path between the source and destination. The information regarding the medium state at the PHY layer is extracted in the form of the probability of the bit error and then mapped into the packet error probability at the MAC layer. Furthermore, the packet error probability is utilized for the estimation of the bit rate per channel, which is used in the dynamically scaled threshold for the selection of the next hop station.

Performance analysis of an improved adaptive routing and fixed routing algorithm in the BPLC access network is completed using the cross-layer BPLC simulator BPlcSim [6]. Simulations of both routing algorithms are performed on the model of the realistic LV PLC network defined within the European research project DLC+VIT4IP [7]. Comparison of the routing algorithms is based on the values of the quality of service (QoS) parameters.

A state-of-the-art overview of the existing MAC routing algorithms for the BPLC network is presented in Section 2. Since the adaptive algorithm employs the infrastructure of the IEEE P1901 standard, a short description of the standard is provided in Section 3. The concept of the BPlcSim and the adaptive routing algorithm is described in Sections 4 and 5, respectively. Simulation results are presented in Section 6 and the conclusion in Section 7.

2. MAC layer routing algorithms in the BPLC network

The majority of the available MAC layer routing algorithms in PLC systems are intended for smart metering purposes. In most cases, only two approaches have been utilized for the development of such algorithms. The first is the clustering approach, where stations in the network are grouped according to a predefined rule. Each station in the cluster communicates through the cluster head, which performs the routing and repeating functions. The routing algorithm of Wang et al. is based on an overlapping clustering algorithm by classification of the nodes into logical layers during the initialization process [8]. The major advantage of this approach is the existence of multiple paths for a same destination. A new MAC routing algorithm based on the minimum identification (ID) clustering algorithm was presented in [9]. The station in the cluster that is the closest to the gateway is selected to serve as a repeater. Tangential clustering algorithms can also be used for the development of the MAC routing algorithm [10]. The algorithm in [10] differs from the other clustering algorithms in that each station in a layer can communicate with the head cluster through any station in the same layer using the tangential connections. These mentioned cluster-based MAC routing algorithms do not analyze the influence of multipath signal propagation in the PLC network or noise fluctuations, and neither do they consider the utilization of the different digital communication techniques and the utilized frequency spectrum. They also do not take into consideration any of the existing PLC standards.

The second approach for the development of MAC routing algorithms is founded on the ant colony algorithm [11,12]. According to this algorithm, all nodes operate independently and the node address is provided through the pheromone data. The routing in the network is distributed and its application is limited to small networks. Additionally, each node has to discover the network topology by itself.

Information about the physical PLC device location can be utilized for routing purposes [13]. This so-called geo-routing is based on the prior knowledge of the network topology and the instantaneous information about the neighboring devices. Using this approach signal power is adapted in accodance with the packet destination. The main drawback of this algorithm is high sensitivity to neighboring network changes and direct correlation between the size of the network and the routing packets.

Since the characteristics of the wireless and PLC channel are similar, the authors of [5] analyzed the application of the wireless routing and repeating techniques for the PLC channel. Performance analysis of the three MAC layer packet relay techniques was completed: fixed, channel adaptive, and automatic repeat-request. The results showed that the channel adaptive relay technique is the most effective since it is based on the current channel state. The PLC channel was modeled in accordance with the approach presented in [14,15].

The centralized routing algorithm for the BPLC access network was utilized in [16]. Bandwidth-guaranteed routing and time-slot assignment techniques were analyzed in order to minimize the static bandwidth allocation and maximize the network resource usage. A centralized system for the allocation assignment was utilized. However, the authors did not provide any information regarding the model of the physical network (frequency range, cable attenuation, noise, and multipath effect), and neither did they consider any of the existing PLC standards. The transmission rates between nodes were above 200 Mbps, which is unrealistic for this kind of multihop network. Furthermore, channel reuse technique was employed in order to increase the link rate. Additionally, they did not provide an algorithm that enables the node to detect when and if such a technique is feasible in the networks.

Another routing algorithm for the PLC network was considered in [17]. The multiobjective combinatorial optimization problem of planning and routing was analyzed and information necessary for the selection of the access nodes and repeaters was determined. However, the algorithm in [17] does not consider the influence of the impulsive noise, signal multipath propagation, and existing PLC standards [7].

The foundations of the analyzed MAC routing algorithms presented in this paper are defined within the P1901 standard [3]. The selection of the next hop station in the packet routing process is performed on the basis of the estimated effective bit rate between the stations at the PHY layer. In this way, the information from the PHY layer is used for the MAC packet routing.

3. MAC layer description by IEEE P1901 standard

The IEEE P1901 is a comprehensive standard for the MAC protocols in the access and in-home PLC networks [3]. According to the IEEE P1901 standard, the PLC network is divided into cells. The cell is a set of stations, where each station implements one of the following roles: head end (HE), repeater (RP), or network termination unit (NTU). The HE provides the means of the admission control through the periodic emission of the beacons, which carries information regarding the time slots in which stations can access the medium using one of two available mechanisms. The first mechanism is based on carrier sense multiple access with collision avoidance (CSMA/CA) and is reserved for the transmission of packets with lower QoS requirements. The IEEE P1901 uses a refined CSMA/CA algorithm based on the channel access priority (CAP). Furthermore, there are two schemes implementing this mechanism, known as priority resolution symbol (PRS) and interframe spaces (IFS). In the PRS scheme, intent for channel access is expressed by the emission of two priority resolution symbols that correspond to the four types of CAP denoted as CA_i , $i = 0, 1, 2, 3$. If a station detects a priority higher than the one it has, it defers from sending the PRS and waits for the next CSMA/CA slot. Therefore, the stations with the highest priority remain and contend for the medium access using the random backoff algorithm. Unlike the PRS scheme, IFS prohibits emission of the PRS but rather utilizes different values for the backoff algorithm in accordance with the CAP.

The second channel access mechanism is time division multiple access (TDMA), which provides the means of achievement of high QoS requirements in the BPLC networks. Utilization of the TDMA mechanism requires connection establishment through the HE station. Newly accepted connections and their allocations are

announced by the HE through the emission of the channel access schedule in the beacons. Efficient utilization of the medium in the TDMA slots is achieved through the technique of a packet bursting, where multiple packets are transmitted in the burst before the medium is released. Connection tear-down is performed under the authority of the HE.

According to the IEEE P1901, a station can be involved in the network traffic activity after it joins the network. When a station powers on, it scans the beacons for a predefined amount of time. A station collects information from beacons about the channel access schedule and the effective bit loading estimate ($EBLE$) upstream and downstream for each station it can hear. The $EBLE$ represents the effective number of data bits per microsecond that can be carried by each channel. Using this information, the station selects the next hop station (NHS) for communication with the HE. The NHS is the station with the maximum $EBLE$ in downstream towards the HE ($EBLE\_DOWN$). For station n seeking a NHS and a given station k, $EBLE\_DOWN$ is [3]:

$$EBLE\_DOWN_n = \frac{1}{\frac{1}{EBLE\_DOWN_k} + \frac{1}{BLE_{nk}}} \tag{1}$$

where $EBLE\_DOWN_k$ is the $EBLE$ in downstream for station k and BLE_{nk} is the bit loading estimate (BLE) between stations n and k, calculated as:

$$BLE = \frac{N_b \cdot R \cdot (1 - p_{PB})}{T_s} \tag{2}$$

where N_b is the number of data bits per OFDM symbol, R is the forward error correction (FEC) code rate, T_s is the OFDM symbol length including the cyclic prefix, and p_{PB} is the packet error probability at the PHY layer. After the station has selected the NHS, the process of association is initiated and the HE assigns the terminal equipment identifier (TEI) address to the station. Afterwards, the station with the new TEI address initiates the process of route establishment where stations towards the HE update their routing tables with the TEI address of the newly associated station. The process of joining the network is finished after successful completion of the authorization and authentication procedures.

The IEEE P1901 standard employs the algorithm for selective acknowledgement (SACK) for reliable packet delivery. Each time a station emits a packet, the SACK algorithm initiates the timer. If the acknowledgement arrives before the time-out event, the packet is discarded from the queue and the timer is reset. Otherwise, retransmission of the packet is performed and the timer is initiated again.

In its core, the IEEE P1901 standard provides the infrastructure for the implementation of the two routing and repeating algorithms: the basic approach (BA) and distance vector (DV). The BA routing algorithm is established with the assumption that all communication goes through the HE. Therefore, only the HE knows the address of all stations in the network and the set of TEI addresses on the path toward each station. Repeaters keep the addresses of the stations they serve as the next hop toward the HE. Selection of the NHS is based on the algorithm that maximizes the $EBLE$ downstream and minimizes the BL. The BA routing algorithm results in the same downstream and upstream routes. The DV routing algorithm assumes that in the point-to-point communication an end-point station is not necessarily a HE. In the DV approach, each station maintains information about all stations in the network. Stations periodically exchange routing information in order to update the routing table.

4. Architecture of the cross-layer based BPLC simulator BPlcSim

The BPlcSim simulator enables simulation of the cross-layer interaction between the MAC and PHY layers in the BPLC network [6]. The BPLC system performance at the MAC layer is influenced by PLC channel characteristics and digital communication techniques such as modulation and channel coding at the PHY layer. The probability of bit error is a function that correlates PHY with MAC layer and can be utilized for the implementation of this interaction. This fact is crucial for the concept of the proposed simulator. The simulator incorporates two models: the physical layer model (PLM) and the MAC layer model (MLM). The PLM is defined by the three groups of input parameters (Figure 1).

The first group of input parameters constitutes the topology matrix (TM), which provides information regarding the position of the stations and branching in the BPLC access network. Furthermore, the TM includes cable parameters and station input impedances. Using the four-port network described by A parameters [14,15] and the TM, the frequency response for each pair of stations in the network and their appropriate impulse response is calculated (Figure 1).

The same approach is applied to each pair of stations and branching points in order to calculate the signal attenuation at all branching points. This information is forwarded to the MLM for making the decision about the possible packet discarding at the branching points when the signal drops below the power threshold determined by the receiver sensitivity.

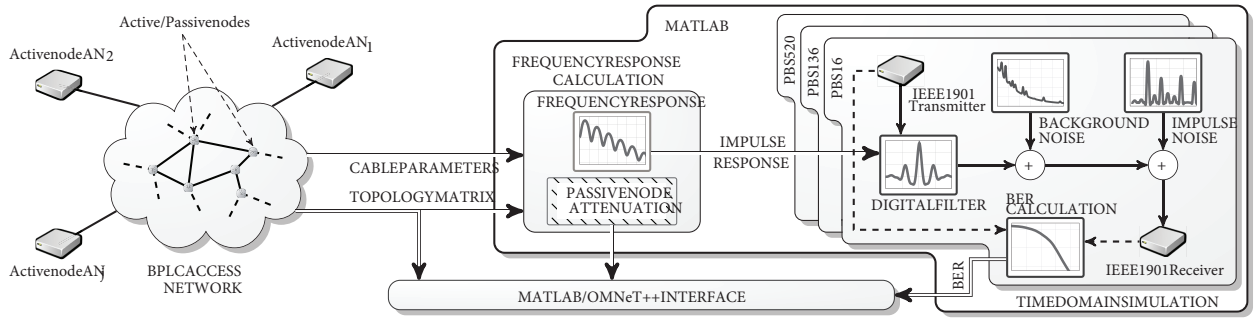

Figure 1. The physical layer segment of the simulator implemented in MATLAB with emphasized PHY layer block sizes (PBS = 16, 136, 520).

The second group of input parameters refers to the noise level in the network. Generally, the noise in the PLC can be categorized into five types [18]. However, the PLM noise model is simplified and includes generalized background and aperiodic impulse noise [19]. The generalized background noise (GBN) model incorporates colored background noise $N_{CBN}(f)$ and noise generated from narrowband disturbers $N_{ND}(f)$ [19]. The power spectral density of the colored background noise can be expressed as in [20]:

$$N_{CBN}(f) = -35 + 35e^{\frac{f[MHz]}{3.6}} \left[\frac{dB\mu V}{Hz}\right] \tag{3}$$

and the power spectral density of the narrowband disturber as in [19]:

$$N_{ND}(f) = \sum_{k=1}^{N_1}\sum_{n=1}^{N_2} A(k,n) exp\left(-\frac{(f - f_0(k,n))^2}{4B^2(k,n)}\right) \left[\frac{dBm}{Hz}\right] \tag{4}$$

where N_1 is the number of frequency subbands, N_2 is the number of disturbers in each frequency subband, and f_0 and B are central frequency and bandwidth of disturbers while A defines the relative power gain of

the narrowband disturber compared to the background noise power. In the model for the impulse noise (IN) we assume that the arrival of the impulses follows the Poisson process [21,22] with the rate λ, in the manner that k arrivals in T seconds has the probability density function of

$$p(k) = e^{-\lambda T} \frac{(\lambda T)^k}{k!} \tag{5}$$

Total average duration of the impulse noise T_{TIN} in the time interval of T seconds, when the average duration of impulse noise is T_{IN}, can be calculated as in [22]:

$$T_{TIN} = \sum_{k=0}^{\infty} k T_{IN} e^{-\lambda T} \frac{(\lambda T)^k}{k!} = T_{IN} \lambda T. \tag{6}$$

The third group of input parameters is provided by the IEEE P1901 standard and defines the applied modulation and coding techniques. These three groups of parameters enable the calculation of the bit error probability for each pair of stations in the network using the Monte Carlo simulations in MATLAB (Figure 1).

The PHY layer packets are represented by the PHY layer data blocks (PB). The PHY layer data block size (PBS) defines the number of data bytes (16, 136, or 520) that is being carried by the PB (Figure 1). Each PB is composed of a few OFDM symbols modulated and coded using different communication techniques. These interchanges in the modulation and coding techniques in the OFDM symbols for the particular BPLC access networks with N stations require computation of $3N(N-1)/2 \quad p_e = f(SNR)$ functions. Calculation of $p_e = f(SNR)$ for each channel and PBS combination is performed in two stages. In the first stage, the probability of bit error p_{BN} is determined for the channel with the background noise. The probability p_{BN} is calculated by simulating the transmission of D_{BN} data bits. Before emission, data bits are grouped in accordance with the PBS, scrambled, and coded using the double binary turbo code with code rate 1/2. Furthermore, bits are interleaved using the 4-stage channel interleave and modulated using the BPSK or 16 QAM modulation technique, depending on the PBS. The resulting symbols are loaded on 917 OFDM carriers out of 2048 available OFDM carriers spread over the frequency range (0, 30) MHz [3]. In this way, D_{BN} data bits are mapped into C_{BN} OFDM symbols. The OFDM symbol interval T_{OFDM} is $40.94\,\mu s$ long plus the cyclic prefix of $7.56\,\mu s$. The emission process of D_{BN} data bits requires $C_{BN}T_{OFDM}$ seconds. During this time interval, the average duration of the overall impulse noise can be calculated as

$$T_{TIN} = T_{IN} \lambda C_{BN} T_{OFDM} \tag{7}$$

In the second stage, probability of bit error p_{IN} is determined under the influence of IN. The probability p_{IN} is calculated by simulating the transmission of D_{IN} data bits. The D_{IN} data bits are mapped into C_{IN} OFDM symbols, with duration T_{TIN} seconds. Finally, the probability of the bit error for the particular PLC channel and given PBS is calculated as

$$p_e = \frac{p_{BN} D_{BN} + p_{IN} D_{IN}}{D_{BN} + D_{IN}} \tag{8}$$

where the D_{BN} and D_{IN} represent the number of transmitted data bits in the PLC channel, which are influenced only by GBN and IN, respectively. The interaction between the PLM and the MLM is achieved through the interface that contains the TM, a set of $p_e = f(SNR)$ functions for different PBS, and set of branching attenuations. The family of $p_e = f(SNR)$ functions, simulated in MATLAB, are further forwarded to the MAC layer simulator. This provides the necessary interaction between the MAC and PHY layers.

The MLM is implemented using the discrete event simulation framework OMNeT++ [23]. The MLM of the BPLC network is created with the active and passive nodes implemented as a simple module in OMNeT++ [6]. The active node (AN) corresponds to a station in the network and the passive node (PN) to a cable branching (Figure 2). Each AN is always connected to one PN. Furthermore, all nodes in the MLM network are connected with OMNeT++ links in accordance with the TM. The links in the MLM exclusively model the channel delay.

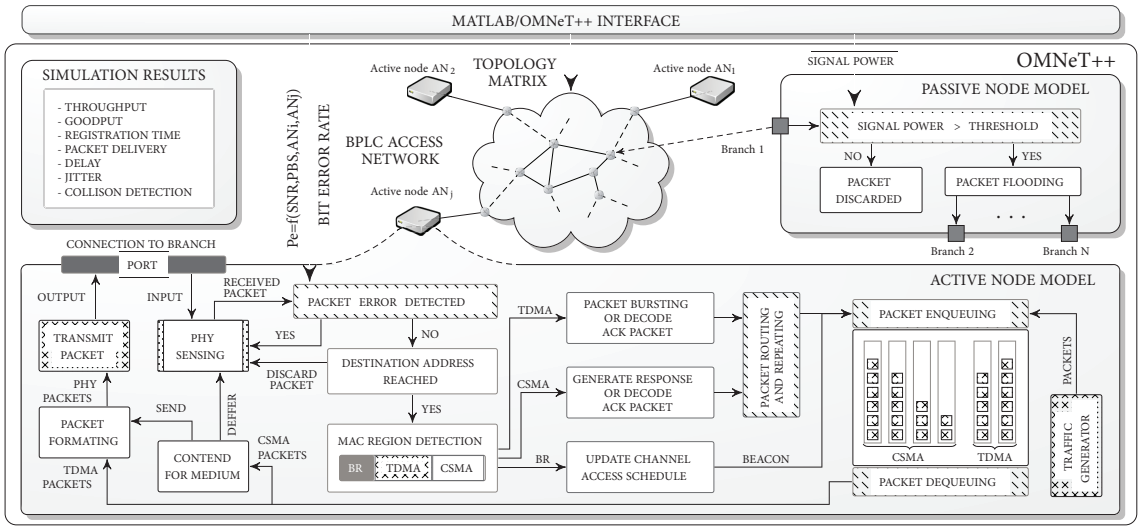

Figure 2. MAC layer segment of the BPlcSim simulator implemented in OMNeT++.

The PN model is designed to simulate the packet flooding in the network by the simple replication of the received packet (Figure 2). An additional functionality of the PN is the inspection of the packet signal power level. When the packet arrives to the PN, the packet signal power is compared with the receiver sensitivity. If the packet signal power is lower than the receiver sensitivity, the packet is discarded and the flooding function is canceled. The packet signal power level inspection is necessary in order to avoid unrealistic channel occupation.

The processing core of the MLM is the AN model generating all packets. The traffic monitoring and PHY sensing in the AN model is achieved through the input/output port (Figure 2). When the packet arrives to the AN, the packet error function is executed. Each packet carries information regarding the source and destination as well as the PBS. Using this information, the AN selects the appropriate $p_e = f(SNR)$ function and calculates the packet error probability p_p from the bit error probability [24]:

$$p_p = 1 - (1 - p_e)^{8 \cdot PBS} \tag{9}$$

In the AN, a random number $p_u \epsilon (0, 1)$ is generated in compliance with the uniform distribution. If p_u is lower than p_p, the received packet is discarded. The correctly received packets are classified by destination address and further processed in accordance with the active region [3]. Region resolution is based on the CAS, which is collected from the beacon packets. In the beacon region, a beacon is transmitted. Each time a new CAS is received, a new beacon is generated and sent into the CSMA queue for transmission (Figure 2).

The packets received in the CSMA region usually carry network management information regarding network status or data with lower QoS requirements. The payload of these packets is analyzed (Figure 2) and an appropriate response is generated. The response can be data or management packets that are enqueued for

transmission in accordance with their priority. In the CSMA region, the AN will tend to send the packets using the CSMA/CA mechanism from the queue with the highest priority. Before the actual packet is sent, the AN has to contend for the medium access and win using the CSMA/CA algorithm. In the TDMA region, only data or ACK packets are transmitted. However, the AN will send packets from the TDMA queue if there is an active connection (Figure 2). Otherwise, the AN will wait for the next time slot. Each packet, regardless of the active region, is formatted before sending in accordance with the IEEE P1901 standard (Figure 2).

The buffer size B for the CSMA and TDMA traffic is designed in accordance with the general rule defined in [25]:

$$B = \frac{2CT}{\sqrt{N}} \tag{10}$$

where C is the link rate, T is one-way link delay, and N is the number of flows.

5. An improved adaptive MAC routing algorithm

The proposed adaptive MAC routing algorithm uses the concept where each station can perform function of a router. Therefore, each station can select its own NHS on the path towards the destination. In the fixed BA routing algorithm integrated within the IEEE P1901 standard, each station in its routing table stores the MAC and the TEI address, beacon level, and hop count to HE for all stations for which they serve as the next hop station to HE (Figure 3). Additionally, the list of all stations that can be reached by a given repeater that uses this station as the next hop station to HE is also stored [3]. For the example presented in Figure 3, this means that stations S_{n+3} and S_{n+4} can be reached via station S_{n+1}.

In accordance with the fixed routing algorithm, the next hop station to HE is changed whenever a station with the higher $EBLE\_DOWN$ value is detected. Due to noise fluctuations in the PLC channel and the hard decision logic for the selection of the next hop station, more frequent selections of the next hop station are likely to occur. As a consequence, the number of management packets, used for the route update, will increase during that time. The difference between the $EBLE\_DOWN$ values for the old and new NHS is usually small and more likely to last for a short period of time. In order to reduce the unnecessary interchange of the NHS as well as the generation of management packets for the route update, in the adaptive routing algorithm we introduce the new dynamically scaled threshold for the selection of the NHS. The new $EBLE\_DOWN$ threshold for the selection of the NHS is the $EBLE\_DOWN$ value of the current NHS scaled by δ.

Whenever the station decides to change the NHS in the fixed routing algorithm, the route update packet is transmitted towards to new NHS. The new NHS updates its routing table and checks if the content of the routing table is changed. If the table is changed, the route update packet is emitted to its own NHS. The procedure continues until the station on the path to HE detects that its routing table did not change after the update [3]. The old NHS holds the information about the stations to which packets are forwarded. The problem occurs when the route update of the old NHS is initiated, implying that routing information reaches the HE. After the route update of the HE, the routing table will contain two paths for the same station, which will result in packet loss due to the false path information.

Within the adaptive routing algorithm we introduce an additional field in the route update packet, named the route update reason code. The value of the reason code field can be an *add* or *delete* route. By using this new field the station can distinguish the case when the received routing information is to be added to or deleted from the routing table. Additionally, the station that initiates the procedure for the selection of the new NHS also must transmit the route update to the old NHS with a reason code set to delete old route.

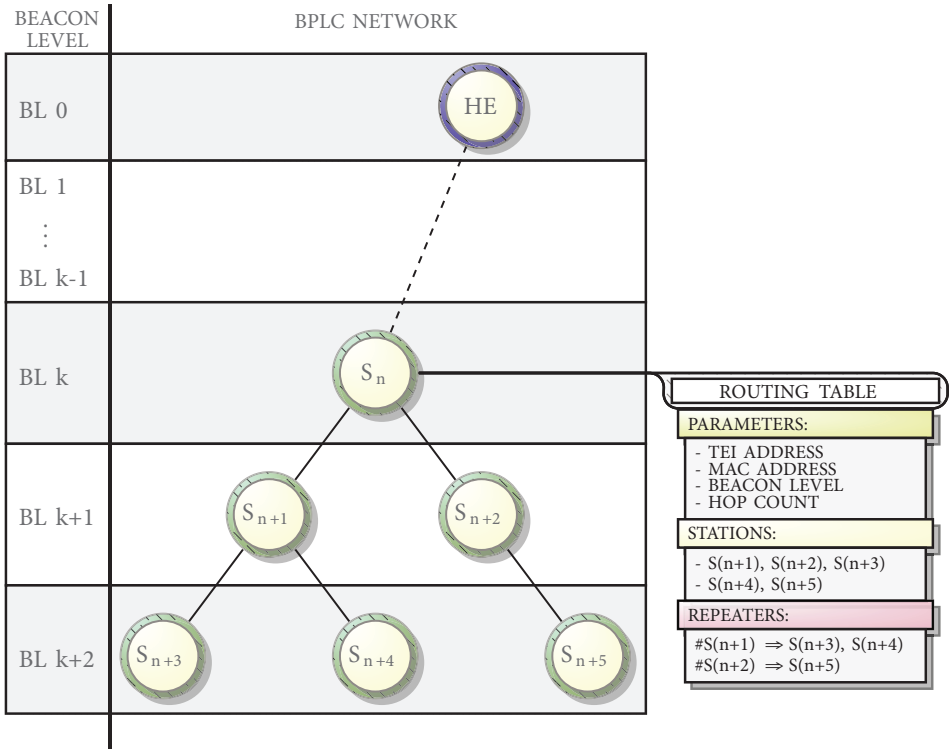

Figure 3. Routing table in the BA algorithm.

The process of routing during the connection setup and maintenance is in direct correlation with the allocation setup procedure. The IEEE P1901 standard supports a centralized and distributed algorithm for the TDMA allocation setup during the connection setup [3]. In the case of centralized allocation setup from the HE standpoint, this means that the HE must have the knowledge of the number of stations on the path to the station that initiated the TDMA connection as well as their addresses. The fixed routing algorithm in the IEEE P1901 standard in the procedure of the TDMA allocation setup suggests that the allocations become valid in the moment when they are successfully transmitted. The allocation setup procedure does not take into account the fact that the route to a station that initiated the TDMA connection could change during that time. The omission of this information may lead to the assignment of TDMA allocation to a station that is not on route to the station that initiated the TDMA connection.

In a case of the adaptive routing algorithm, the allocations become valid from the moment when the HE receives the acknowledgment that the station that initiated the TDMA connection has received TDMA allocations. Otherwise, if one of the stations on the route toward the station that initiated TDMA connection detects that the route has changed the TDMA allocation, setup is canceled and the new TDMA allocation has to be assigned by the HE. The advantage of such an approach is that unnecessary retention of resources is avoided.

During the transmissions in the TDMA allocations, a station may decide to change the NHS. As a result, an additional TDMA allocation has to be requested and granted by the HE [3]. The fixed routing algorithm does not provide the procedure for the modification of the TDMA allocation when the route is changed. However, in our improved adaptive routing algorithm, we have included the mechanism for the route modification during the TDMA connection. In the proposed algorithm when the station on route toward the HE, which is used in the TDMA connection, detects that the NHS is changed, the connection is temporarily paused. The consequence

is that a TDMA allocation packet with the reason code *route changed* is sent to the HE and to the station that initiated the TDMA connection. The stations that participated in the TDMA connection will terminate the transmission of the traffic. Furthermore, all stations on the old route, except the HE, are forced to delete the connection and their TDMA allocations and continue transmission of the remaining traffic in the CSMA allocations. When the HE receives the request for the TDMA allocation modification during the TDMA transmission, the allocations for the old route are deleted and the new allocations are set up.

6. Simulation

6.1. Setup

Performance analysis of the existing fixed and new adaptive routing algorithm has been completed for the actual scenario (Figure 4) defined within the EU research project DLC-VIT4IP [7]. Station S1 in Figure 4 plays the role of the HE. The number of stations that perform the routing and repeating (RR) functions in the fixed routing scenario equals three in order to reach station S16 (Figure 4).

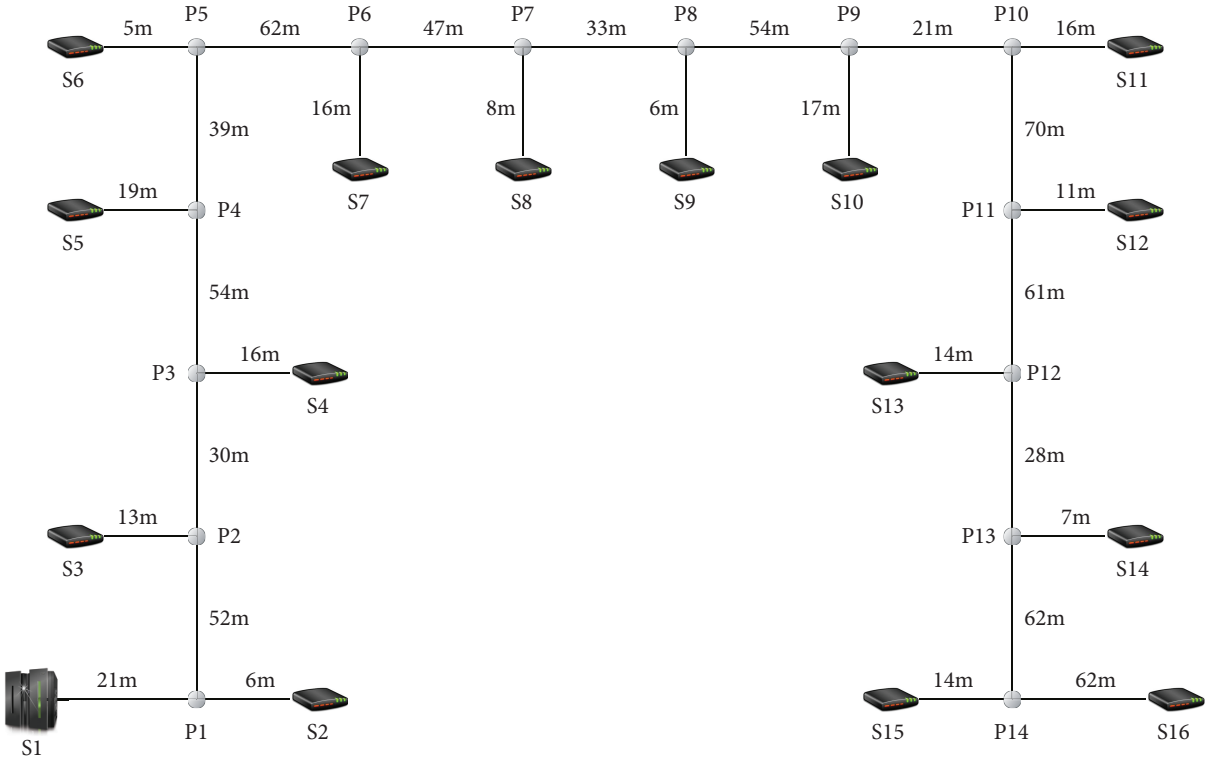

Figure 4. Topology of the test LV PLC access network [7].

In the fixed routing scenario, the RR stations are approximately equally distanced from each other. Furthermore, stations S5, S9, and S13 are selected as repeaters in the fixed routing scenario. On the other hand, each station can perform the RR function in the adaptive routing algorithm.

The input and output impedances of the stations are equal to the characteristic impedance of the cable. The cable parameters are also adopted from [7] and presented in Table 1.

The transmitted signal power is limited to 21.5 dBm using the default tone mask (Figure 5, on the left side) defined within the IEEE P1901 standard [3]. The generalized background noise power spectral density

(PSD) is depicted in Figure 5 (right side). The narrowband noise N_{ND} is divided into the three frequency subbands (0, 10) MHz, (10, 20) MHz, and (20, 30) MHz with five, three, and two disturbers, respectively. The parameters of central frequencies f_0 bandwidth B, and relative gain A of the narrowband disturber are created with the algorithm presented in [19] and presented in Table 2.

Table 1. Transmission line parameters of power cables.

Parameter	$R^{'}[m\Omega/m]$	$\mu L^{'}[H/m]$	$C^{'}[pF/m]$	δ
Value	0.268	0.356	1.560	0.004

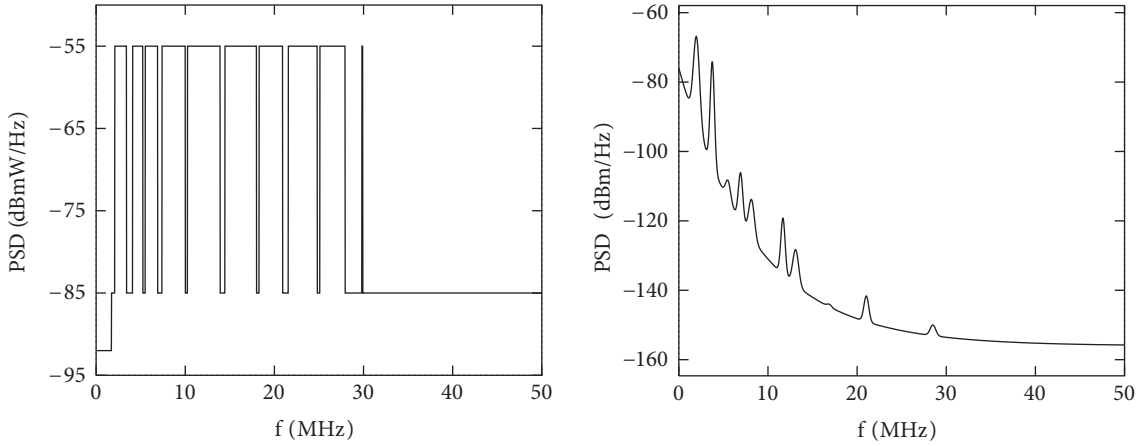

Figure 5. Spectral tone mask (left) and PSD of the background noise model (right).

The impulse noise parameters are adopted from [18]. The impulse rate λ in Eqs. (5) and (6) is set to $1.08\,s^{-1}$, average impulse duration T_{TIN} is $46.5\,\mu s$, and relative impulse noise power is $31.5\,dB$ higher than the background noise power.

The buffers in the MAC layer model are designed for the worst case scenario regarding Eq. (10), valid for the number of flows equal to one. Additionally, we made an assumption that the one-way link delay is not higher than 100 ms. The maximum link rate that the station can utilize depends on the communication techniques at the physical layer, such as modulation and coding techniques, etc. The size of CSMA and TDMA buffers are set to 128 kB and 64 kB, respectively.

Table 2. Parameters for the narrowband disturber noise.

	k/n	1	2	3	4	5
A [dB]	1	25.5230	30.1315	5.5028	14.1036	11.1519
	2	16.2025	10.2679	0.7460	0	0
	3	7.4335	3.0958	0	0	0
$f_0\,[MHz]$	1	1.9879	3.7589	5.5267	6.9318	8.1593
	2	11.6841	13.1106	16.8944	0	0
	3	21.0356	28.5061	0	0	0
$B\,[MHz]$	1	0.3499	0.2350	0.2867	0.2515	0.3295
	2	0.2394	0.3295	0.2585	0	0
	3	0.2715	0.3104	0	0	0

6.2. Results

For each path between stations S_i and S_j, the frequency response is calculated using the two-port model [14,15]. The amplitude frequency response at some frequencies reaches over –120 dB (Figure 6). In Figure 4, branching points are denoted as P_i and the attenuation between two neighboring branching points is in the range of (–3, –4.5) dB. The frequency responses of the paths between the stations together with the description of the background and impulse noise are further used in the PLM for the calculation of the probability of bit error. The probability of the bit error under the influence of the GBN and impulse noise (GBN + IN) is depicted in Figure 6 (right). The signal to noise ratio for Figure 6 (right) is defined in contrast to the power of the generalized background noise. As can be seen from Figure 6 (right), probability of bit error in the cast of GBN noise has lower values for all packet sizes in comparison to probability of bit error in the cast of GBN + IN. The curves for the probability of bit error tend to saturate due to the existence of selective attenuation in the amplitude frequency response (Figure 6, on the left).

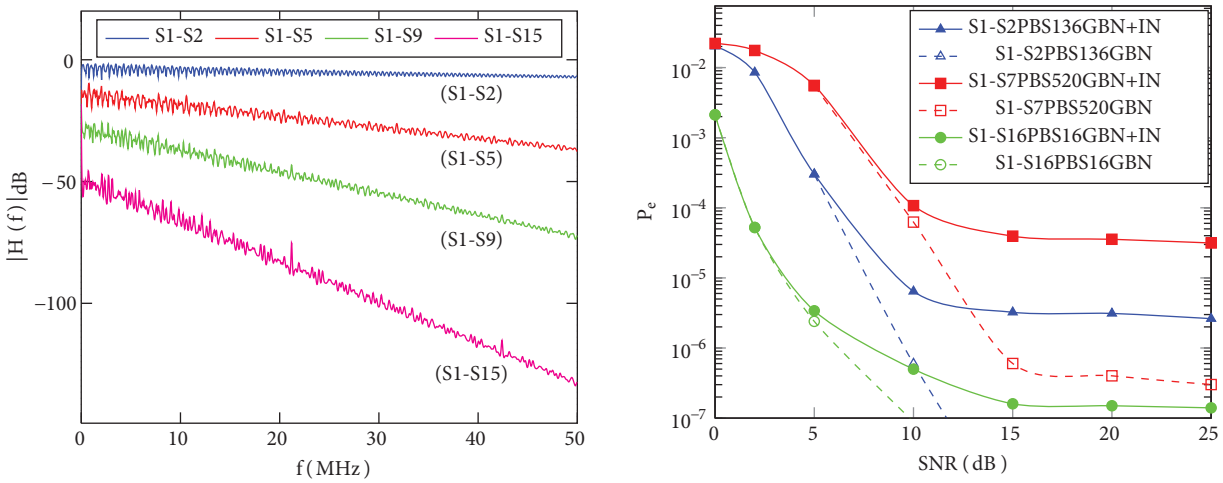

Figure 6. Frequency response of the paths between stations (left) and bit error probability under the influence of the background and impulse noise (right).

One of the parameters that influences the initial selection of the NHS when the station powers on is the minimum number of detected beacons (MNDB). For the adaptive routing algorithm the selection of the MNDB parameter is based on the duration of the registration procedure from the point when all stations are initially unregistered. The results proved that increase of the minimum number of beacons leads to longer registration procedure duration while simultaneously reducing the oscillations of the $EBLE\_DOWN$ value (Figure 7).

The limit for the MNDB before initiation of the registration procedure is in direct correlation with the initial value of the retransmission timer (RTO) and the limit of the retransmission value increment. In order to investigate their influence on the registration time duration, simulations of different combinations of these parameters are performed. The increase of the initial value for the RTO reduces the number of collisions during the registration time (Figure 7, on the left). It can be seen in Figure 7 that when the RTO value is in the multiples of the beacon period, which is in our case 40 ms, the duration of the registration procedure is increased. The main reason for this behavior lies in that all unregistered stations try to access the medium at the beginning of the beacon period. Hence, more collisions occur and the registration timer increases. The increase in the MNDB before initiation of the registration procedure leads to an increase in the registration time

duration (Figure 7, on the right). As a consequence, the number of emitted route update packets is decreased in comparison to the case with lower value of MNDB.

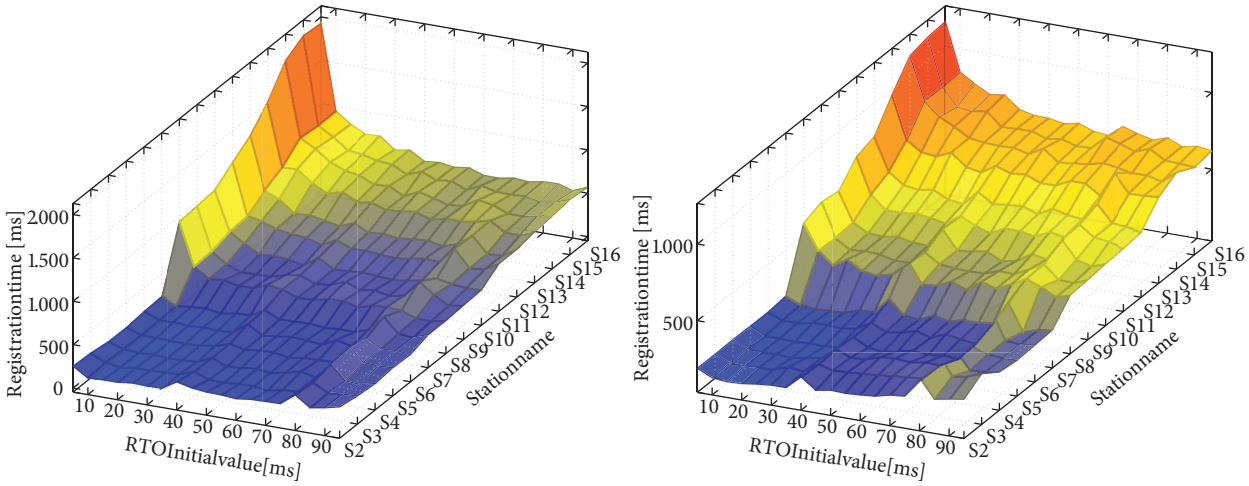

Figure 7. Registration time duration when MNDB equals two (left) and MNDB equals three (right).

Influence of the new dynamically scaled threshold for the selection of the NHS has been analyzed for a range of parameter $\delta\epsilon(1,2)$. The instantaneous $EBLE\_DOWN$ value of the current NHS for stations S7, S11, and S16 is depicted in Figure 8. The increase of the threshold δ value directly influences the oscillations in the instantaneous $EBLE\_DOWN$ value for the NHS. The number of interchanges of the NHS decreases simultaneously.

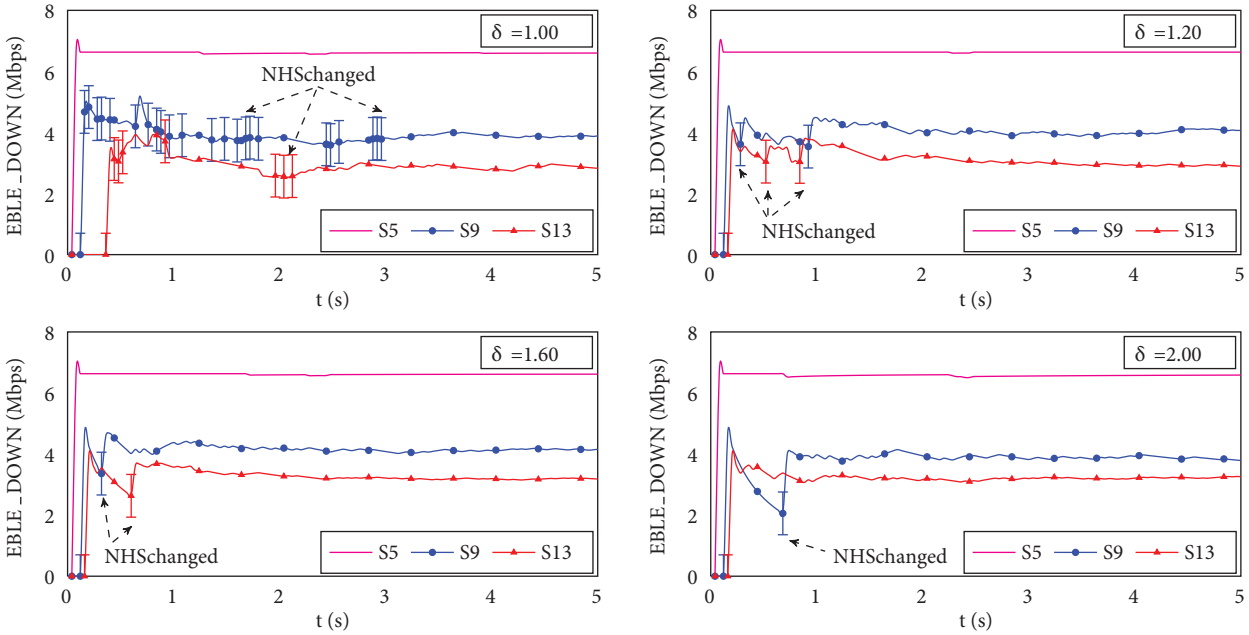

Figure 8. Influence of the EBLE threshold on the selection of the NHS.

When the δ value is lower, the station tends to change the NHS more frequently and the instantaneous $EBLE\_DOWN$ value of the selected NHS has lower oscillations. As a result, these oscillations in the

$EBLE\_DOWN$ value will degrade the QoS parameters of the station. In the following simulations, the value of δ is set to 1.35, the MNDB before initiation of the registration procedure is set to 3, the initial value for the retransmission timer is set to 30 ms, and the limit for the retransmission timer increment is set to 90 ms.

After the parameters for the NHS selection are tuned, we investigate the performance of the two routing techniques from the perspective of QoS parameters. First we analyze their performance regarding the total registration time (TRT). This parameter represents the time interval starting from the moment when the station powers on and ending with the completion of the authentication procedure. The results in Figure 9 show that the average TRT in the case of the adaptive routing is lower for the stations using the RR station. The main reason for the longer duration of the registration procedure in the fixed routing scenario is that the station that requires the RR cannot initiate the registration procedure before the RR station is registered. In the case of adaptive routing, each station that requires the repeater can utilize any registered neighboring station as a repeater and thus execute the registration procedure faster.

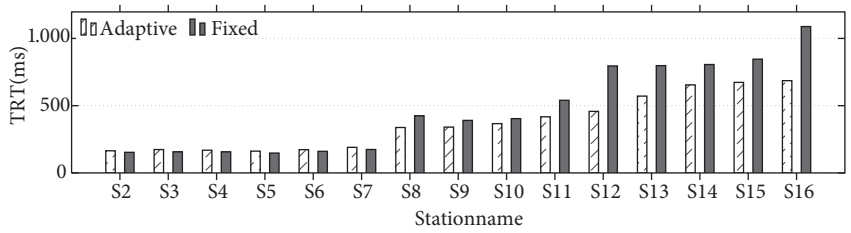

Figure 9. Average total registration time (TRT).

QoS parameters are obtained using the comprehensive simulations performed after all stations have been successfully registered. For the sake of clarity, the first beacon level (BL) group represents the group of the stations (S2–S7) in the direct range of communication with the HE, the second BL group is the group of stations (S8–S11) that requires one repeater in order to communicate with the HE, and so forth. Stations S12–S16 represent the third group. Station S16 in the case of fixed routing requires three repeaters and represents the fourth BL group.

The simulations of one-way delay and jitter in the test BPLC network (Figure 4) are performed in accordance with the procedure defined in [26]. Delay and jitter for both routing approaches are computed for the worst-case scenario corresponding to the situation where all stations equally compete for the medium and the best-case scenario where one station sends the highest priority traffic while other stations idle. Actual delay and jitter values are in the range between the values in the best-case and worst-case scenarios. The results for the delay and jitter are depicted in Figures 10 and 11.

The delay in the worst-case scenario is approximately equal for all stations in the first BL group for both routing algorithms. This is due to the fact that all stations in the first BL group directly communicate with the HE. Furthermore, the delay of the stations in the second and third BL group is higher for the fixed routing in comparison with the adaptive routing. The main reason for this difference can be found in the fact that all packets from the stations in the second and higher BL groups have to pass the same repeater. For the best-case scenario, the delay and the jitter are approximately equal.

The throughput R_b and goodput G_b [24] are simulated for the packets emitted in the TDMA and CSMA region for the best-case and worst-case scenarios (Figures 12 and 13).

The traffic is generated from stations towards the HE. For both routing algorithms, the simulated throughput and goodput in the CSMA and TDMA regions is higher for the stations in direct communication

with the HE. In the CSMA region, the stations cannot fully utilize the medium due to the collisions and the random backoff value, and consequently cannot reach the maximum throughput (Figure 12).

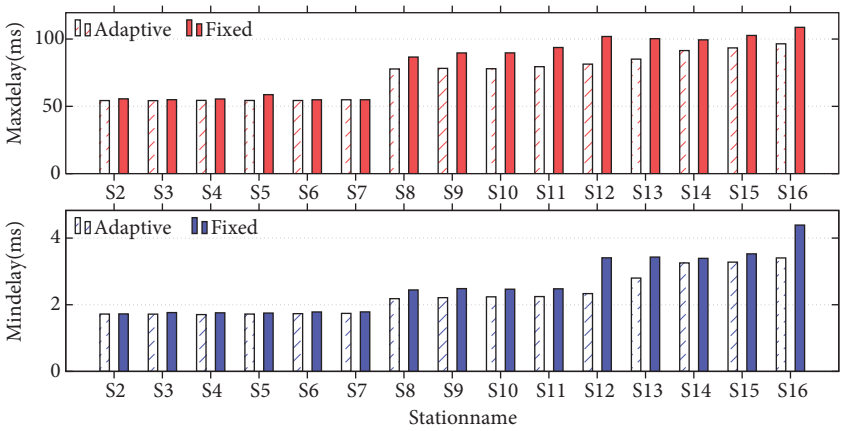

Figure 10. One-way delay in worst-case (top) and best-case scenario (bottom).

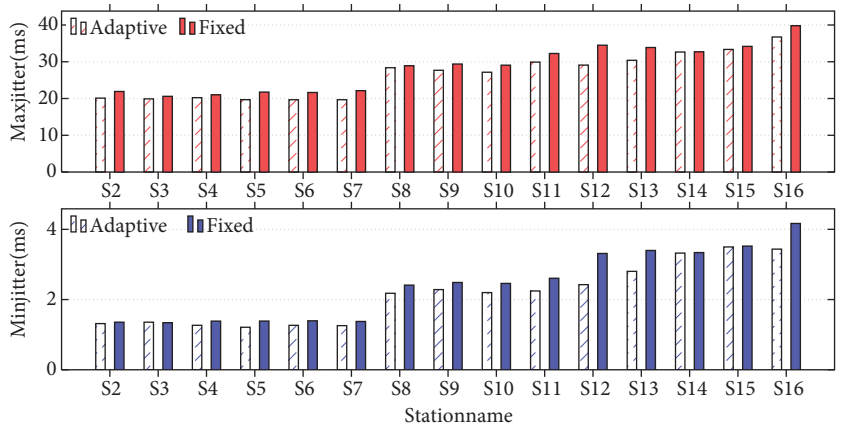

Figure 11. Average jitter in worst-case (top) and best-case scenario (bottom).

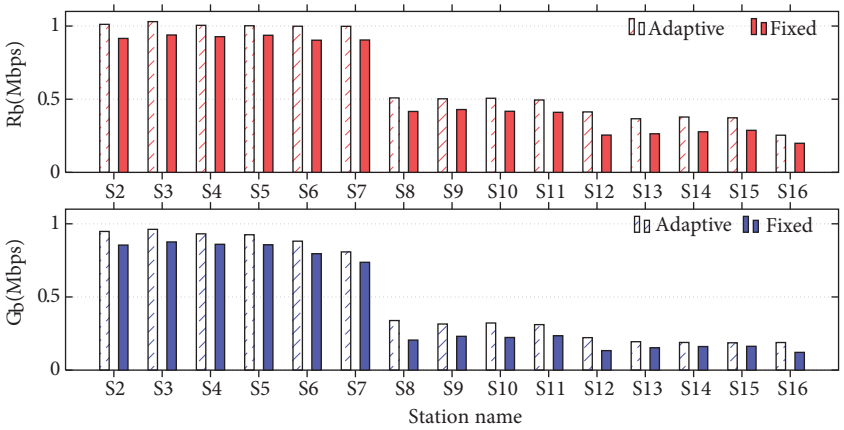

Figure 12. Simulated average throughput and goodput during the CSMA allocations.

On the other hand, in the TDMA region, stations can totally and efficiently utilize the medium. Our conclusion is that the throughput for a station with beacon level k will be k times lower than the throughput of

a station with beacon level one for both of the routing algorithms. Furthermore, the throughput and goodput in the case of the fixed routing algorithm is slightly lower when compared to the results in the adaptive routing, due to the existence of the bottleneck stations.

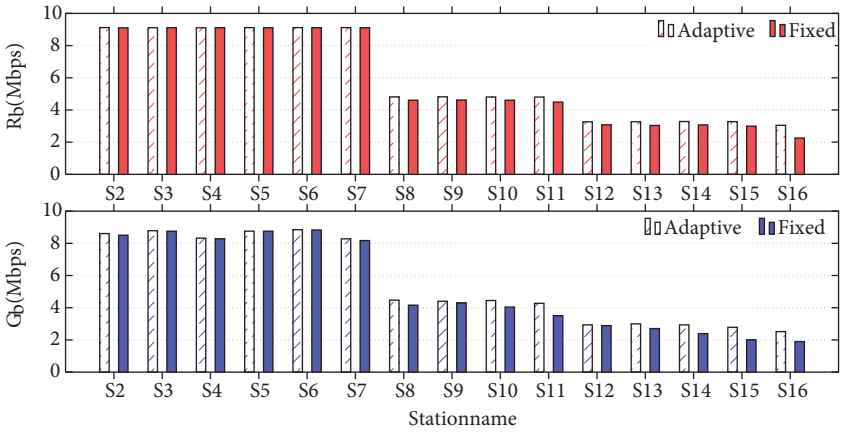

Figure 13. Simulated average throughput and goodput during the TDMA allocations.

Another finding during the simulation of our adaptive routing algorithm is that the probability of packets dropped due to the buffer overflow during the TDMA connection is lower in comparison with the fixed routing algorithm. The main reason for higher packet dropping in the fixed routing algorithm is that all packets of stations behind the router go through that same router.

7. Conclusion

In this paper we presented an improved adaptive routing algorithm for a BPLC access network aligned with the IEEE P1901 standard. This routing algorithm is based on the fact that each station can perform the functions of a router. Selection of the NHS at the MAC layer is made using the dynamically scaled threshold of the bit rate per channel. The estimate of the bit rate per channel is provided through the packet error probability, which is calculated from the bit error probability at the physical layer. In such way, an improved adaptive routing algorithm selects the most reliable station as the NHS towards the destination using the interactions between MAC and PHY layers. Additionally, the procedures for the connection adjustment during the route modification are developed.

The simulation results confirmed that the adaptive routing algorithm outperforms the fixed routing since it utilizes the best route in accordance with the state of the network. The advantage of the adaptive routing algorithm is expressed in the shorter registration time of stations, lower delay and jitter, and higher throughput and goodput. The main drawback of the adaptive routing algorithm is in the increased emission of the route update packets during the transient states in the network. On the other hand, the performance of the fixed routing algorithm is degraded even with the lower emissions of the route update packets. The main reason is that all packets have to pass through the same stations, thus leading to congestion and increase in packet delay. Additionally, the probability of buffer overflow during the TDMA connection in fixed routing is much higher.

Acknowledgment

This research was supported by the Scientific and Technological Research Council of Turkey (TÜBITAK) in the scope of the Visiting Scientist's Fellowship Program 2221.

References

[1] Galli S, Scaglione A, Zhifang W. For the grid and through the grid: the role of power line communications in the smart grid. P IEEE 2011; 99: 998–1027.

[2] Güngör VC, Sahin D, Kocak T, Ergüt S, Buccella C, Cecati C, Hancke GP. Smart grid technologies: communication technologies and standards. IEEE T Ind Inform 2011; 7: 529–539.

[3] IEEE P1901 Working Group. IEEE Standard for Broadband over Power Line Networks: Medium Access Control and Physical Layer Specifications. IEEE Standardd 1901-2010. New York, NY, USA: IEEE, 2010.

[4] Zimmermann M, Dostert K. A multipath model for the powerline channel. IEEE T Commun 2002; 50: 553–559.

[5] Lampe L, Vinck AJH. Cooperative multihop power line communications. In: IEEE 2012 International Symposium on Power Line Communications and Its Applications; 27–30 March 2012; Beijing, China. New York, NY, USA: IEEE. pp. 1–6.

[6] Gogic A, Mujcic A, Zajc M, Suljanovic N. Broadband PLC network cross-layer simulation in accordance with the IEEE P1901 standard. Elektron Elektrotech 2013; 19: 83–88.

[7] DLC+VIT4IP Team. Reference Scenario Parameter Specification. Brussels, Belgium: European Community's Seventh Framework Program DLC+VIT4IP, 2010.

[8] Wang Z, Wang YJ, Wang J. Overlapping clustering routing algorithm based on L-PLC meter reading system. In: IEEE 2009 International Conference on Automation and Logistics; 5–7 August 2009; Shenyang, China. New York, NY, USA: IEEE. pp. 1350–1355.

[9] Chenchen H, Younghai H. Study on cluster-based dynamic routing algorithm in power line communication network. In: IEEE 2012 International Conference on Automation and Logistics; 15–17 August 2012; Zhengzhou, China. New York, NY, USA: IEEE. pp. 461–465.

[10] Liu X, Wang W, Zheng J, Hai T, Zhang L, Liu B. Tangential connection clustering routing algorithm for the L-PLC based AMR system. In: IEEE 2012 International Power Electronics and Motion Control Conference; 2–5 June 2012; Harbin, China. New York, NY, USA: IEEE. pp. 2932–2936.

[11] Wang Z, Zhang Y, Zhao Y. A distributed routing algorithm for the L-PLC network. In: IEEE 2008 International Conference on Automation and Logistics; 1–3 September 2008; Qingdao, China. New York, NY, USA: IEEE. pp. 2541–2545.

[12] Liu X, Zhou Y, Qi J. Method study of automatic routing for power line communications. P CSEE 2006; 26: 76–81.

[13] Biagi M, Greco S, Lampe L. Neighboring-knowledge based geo-routing in PLC. In: IEEE 2012 International Symposium on Power Line Communications and Its Applications; 27–30 March 2012; Beijing, China. New York, NY, USA: IEEE. pp. 7–12.

[14] Galli S, Banwell T. A novel approach to the modeling of indoor power line channel - Part II: Transfer function and its properties. IEEE T Power Deliver 2005; 20: 1869–1878.

[15] Tonello AM, Versolatto F. Bottom-up statistical PLC channel modeling - Part I: Random topology model and efficient transfer function computation. IEEE T Power Deliver 2011; 26: 891–898.

[16] Lee SSW, Li KY, Wu CS, Pan JY, Chuang CY. Optimal bandwidth guaranteed routing ant time slot assignment for broadband PLC access network. In: IEEE 2012 International Symposium on Power Line Communications and Its Applications; 27–30 March 2012; Beijing, China. New York, NY, USA: IEEE. pp. 224–229.

[17] Canale S, Giorgio AD, Lanna A, Mercurio A, Panfili M, Pietrabissa A. Optimal planning and routing in the medium voltage power line communication networks. IEEE T Smart Grid 2012; 4: 711–719.

[18] Zimmermann M, Dostert K. Analysis and modeling of impulsive noise in broad-band powerline communications. IEEE T Electromagn C 2002; 44: 249–258.

[19] Andreadou N, Pavlidou FN. Modeling the noise on the OFDM power-line communications system. IEEE T Power Deliver 2010; 25: 150–157.

[20] Hrasnica H, Haidine A, Lehnert R. Broadband Powerline Communications Networks. New York, NY, USA: Wiley, 2004.

[21] Andreadou N, Pavlidou FN. PLC channel: impulsive noise modeling and its performance evaluation under different array coding schemes. IEEE T Power Deliver 2009; 24: 585–595.

[22] Massaki K. Introduction to robust, reliable and high-speed power-line communication systems. IEICE T Fund Electr 2001; 12: 2958–2965.

[23] Varga A. The OMNeT++ discrete event simulation system. In: ESM 2001 European Simulation Multiconference; 6–9 June 2001; Prague, Czech Republic. San Diego, CA, USA: ESM. pp. 319–324.

[24] Cao L, Kam PY, Tao M. Impact of imperfect channel state information on ARQ schemes over Rayleigh fading channels. In: IEEE 2009 International Conference on Communications; 14–18 June 2009; Dresden, Germany. New York, NY, USA: IEEE. pp. 1–5.

[25] Dhamdhere A, Jiang H, Dovrolis C. Buffer sizing for congested Internet links. In: IEEE 205 Joint Conference of the IEEE Computer and Communications Societies; 13–17 March 2005; Miami, USA. New York, NY, USA: IEEE. pp. 1072–1083.

[26] Schulzrinne H, Casner S, Frederick R, Jacobson V. RFC3550 - RTP: A Transport Protocol for Real-Time Applications. Reston, VA, USA: Internet Engineering Task Force, 2003.